Measurement of Time-Dependent CP Asymmetries and the CP-odd Fraction in the Decay $B^0 \to D^{*+}D^{*-}$

The *BABAR* Collaboration

July 24, 2002

Abstract

We present a measurement of time-dependent CP asymmetries and an updated determination of the CP-odd fraction in the decay $B^0 \to D^{*+}D^{*-}$. The measurements are derived from a data sample of $88 \times 10^6 B\bar{B}$ pairs collected by the *BABAR* detector at the PEP-II energy asymmetric B Factory at SLAC. All results are preliminary.

Contributed to the 31st International Conference on High Energy Physics,
7/24—7/31/2002, Amsterdam, The Netherlands

The *BABAR* Collaboration,

B. Aubert, D. Boutigny, J.-M. Gaillard, A. Hicheur, Y. Karyotakis, J. P. Lees, P. Robbe, V. Tisserand, A. Zghiche

Laboratoire de Physique des Particules, F-74941 Annecy-le-Vieux, France

A. Palano, A. Pompili

Università di Bari, Dipartimento di Fisica and INFN, I-70126 Bari, Italy

J. C. Chen, N. D. Qi, G. Rong, P. Wang, Y. S. Zhu

Institute of High Energy Physics, Beijing 100039, China

G. Eigen, I. Ofte, B. Stugu

University of Bergen, Inst. of Physics, N-5007 Bergen, Norway

G. S. Abrams, A. W. Borgland, A. B. Breon, D. N. Brown, J. Button-Shafer, R. N. Cahn, E. Charles, M. S. Gill, A. V. Gritsan, Y. Groysman, R. G. Jacobsen, R. W. Kadel, J. Kadyk, L. T. Kerth, Yu. G. Kolomensky, J. F. Kral, C. LeClerc, M. E. Levi, G. Lynch, L. M. Mir, P. J. Oddone, T. J. Orimoto, M. Pripstein, N. A. Roe, A. Romosan, M. T. Ronan, V. G. Shelkov, A. V. Telnov, W. A. Wenzel

Lawrence Berkeley National Laboratory and University of California, Berkeley, CA 94720, USA

T. J. Harrison, C. M. Hawkes, D. J. Knowles, S. W. O'Neale, R. C. Penny, A. T. Watson, N. K. Watson

University of Birmingham, Birmingham, B15 2TT, United Kingdom

T. Deppermann, K. Goetzen, H. Koch, B. Lewandowski, K. Peters, H. Schmuecker, M. Steinke

Ruhr Universität Bochum, Institut für Experimentalphysik 1, D-44780 Bochum, Germany

N. R. Barlow, W. Bhimji, J. T. Boyd, N. Chevalier, P. J. Clark, W. N. Cottingham, C. Mackay, F. F. Wilson

University of Bristol, Bristol BS8 1TL, United Kingdom

K. Abe, C. Hearty, T. S. Mattison, J. A. McKenna, D. Thiessen

University of British Columbia, Vancouver, BC, Canada V6T 1Z1

S. Jolly, A. K. McKemey

Brunel University, Uxbridge, Middlesex UB8 3PH, United Kingdom

V. E. Blinov, A. D. Bukin, A. R. Buzykaev, V. B. Golubev, V. N. Ivanchenko, A. A. Korol, E. A. Kravchenko, A. P. Onuchin, S. I. Serednyakov, Yu. I. Skovpen, A. N. Yushkov

Budker Institute of Nuclear Physics, Novosibirsk 630090, Russia

D. Best, M. Chao, D. Kirkby, A. J. Lankford, M. Mandelkern, S. McMahon, D. P. Stoker

University of California at Irvine, Irvine, CA 92697, USA

C. Buchanan, S. Chun

University of California at Los Angeles, Los Angeles, CA 90024, USA

H. K. Hadavand, E. J. Hill, D. B. MacFarlane, H. Paar, S. Prell, Sh. Rahatlou, G. Raven, U. Schwanke, V. Sharma

University of California at San Diego, La Jolla, CA 92093, USA

2

J. W. Berryhill, C. Campagnari, B. Dahmes, P. A. Hart, N. Kuznetsova, S. L. Levy, O. Long, A. Lu, M. A. Mazur, J. D. Richman, W. Verkerke

University of California at Santa Barbara, Santa Barbara, CA 93106, USA

J. Beringer, A. M. Eisner, M. Grothe, C. A. Heusch, W. S. Lockman, T. Pulliam, T. Schalk, R. E. Schmitz, B. A. Schumm, A. Seiden, M. Turri, W. Walkowiak, D. C. Williams, M. G. Wilson

University of California at Santa Cruz, Institute for Particle Physics, Santa Cruz, CA 95064, USA

E. Chen, G. P. Dubois-Felsmann, A. Dvoretskii, D. G. Hitlin, F. C. Porter, A. Ryd, A. Samuel, S. Yang

California Institute of Technology, Pasadena, CA 91125, USA

S. Jayatilleke, G. Mancinelli, B. T. Meadows, M. D. Sokoloff

University of Cincinnati, Cincinnati, OH 45221, USA

T. Barillari, P. Bloom, W. T. Ford, U. Nauenberg, A. Olivas, P. Rankin, J. Roy, J. G. Smith, W. C. van Hoek, L. Zhang

University of Colorado, Boulder, CO 80309, USA

J. L. Harton, T. Hu, M. Krishnamurthy, A. Soffer, W. H. Toki, R. J. Wilson, J. Zhang

Colorado State University, Fort Collins, CO 80523, USA

D. Altenburg, T. Brandt, J. Brose, T. Colberg, M. Dickopp, R. S. Dubitzky, A. Hauke, E. Maly, R. Müller-Pfefferkorn, S. Otto, K. R. Schubert, R. Schwierz, B. Spaan, L. Wilden

Technische Universität Dresden, Institut für Kern- und Teilchenphysik, D-01062 Dresden, Germany

D. Bernard, G. R. Bonneaud, F. Brochard, J. Cohen-Tanugi, S. Ferrag, S. T'Jampens, Ch. Thiebaux, G. Vasileiadis, M. Verderi

Ecole Polytechnique, LLR, F-91128 Palaiseau, France

A. Anjomshoaa, R. Bernet, A. Khan, D. Lavin, F. Muheim, S. Playfer, J. E. Swain, J. Tinslay

University of Edinburgh, Edinburgh EH9 3JZ, United Kingdom

M. Falbo

Elon University, Elon University, NC 27244-2010, USA

C. Borean, C. Bozzi, L. Piemontese, A. Sarti

Università di Ferrara, Dipartimento di Fisica and INFN, I-44100 Ferrara, Italy

E. Treadwell

Florida A&M University, Tallahassee, FL 32307, USA

F. Anulli,[1] R. Baldini-Ferroli, A. Calcaterra, R. de Sangro, D. Falciai, G. Finocchiaro, P. Patteri, I. M. Peruzzi,[1] M. Piccolo, A. Zallo

Laboratori Nazionali di Frascati dell'INFN, I-00044 Frascati, Italy

S. Bagnasco, A. Buzzo, R. Contri, G. Crosetti, M. Lo Vetere, M. Macri, M. R. Monge, S. Passaggio, F. C. Pastore, C. Patrignani, E. Robutti, A. Santroni, S. Tosi

Università di Genova, Dipartimento di Fisica and INFN, I-16146 Genova, Italy

[1]Also with Università di Perugia, I-06100 Perugia, Italy

3

S. Bailey, M. Morii

Harvard University, Cambridge, MA 02138, USA

R. Bartoldus, G. J. Grenier, U. Mallik

University of Iowa, Iowa City, IA 52242, USA

J. Cochran, H. B. Crawley, J. Lamsa, W. T. Meyer, E. I. Rosenberg, J. Yi

Iowa State University, Ames, IA 50011-3160, USA

M. Davier, G. Grosdidier, A. Höcker, H. M. Lacker, S. Laplace, F. Le Diberder, V. Lepeltier, A. M. Lutz,
T. C. Petersen, S. Plaszczynski, M. H. Schune, L. Tantot, S. Trincaz-Duvoid, G. Wormser

Laboratoire de l'Accélérateur Linéaire, F-91898 Orsay, France

R. M. Bionta, V. Brigljević , D. J. Lange, K. van Bibber, D. M. Wright

Lawrence Livermore National Laboratory, Livermore, CA 94550, USA

A. J. Bevan, J. R. Fry, E. Gabathuler, R. Gamet, M. George, M. Kay, D. J. Payne, R. J. Sloane,
C. Touramanis

University of Liverpool, Liverpool L69 3BX, United Kingdom

M. L. Aspinwall, D. A. Bowerman, P. D. Dauncey, U. Egede, I. Eschrich, G. W. Morton, J. A. Nash,
P. Sanders, D. Smith, G. P. Taylor

University of London, Imperial College, London, SW7 2BW, United Kingdom

J. J. Back, G. Bellodi, P. Dixon, P. F. Harrison, R. J. L. Potter, H. W. Shorthouse, P. Strother, P. B. Vidal

Queen Mary, University of London, E1 4NS, United Kingdom

G. Cowan, H. U. Flaecher, S. George, M. G. Green, A. Kurup, C. E. Marker, T. R. McMahon, S. Ricciardi,
F. Salvatore, G. Vaitsas, M. A. Winter

*University of London, Royal Holloway and Bedford New College, Egham, Surrey TW20 0EX, United
Kingdom*

D. Brown, C. L. Davis

University of Louisville, Louisville, KY 40292, USA

J. Allison, R. J. Barlow, A. C. Forti, F. Jackson, G. D. Lafferty, A. J. Lyon, N. Savvas, J. H. Weatherall,
J. C. Williams

University of Manchester, Manchester M13 9PL, United Kingdom

A. Farbin, A. Jawahery, V. Lillard, D. A. Roberts, J. R. Schieck

University of Maryland, College Park, MD 20742, USA

G. Blaylock, C. Dallapiccola, K. T. Flood, S. S. Hertzbach, R. Kofler, V. B. Koptchev, T. B. Moore,
H. Staengle, S. Willocq

University of Massachusetts, Amherst, MA 01003, USA

B. Brau, R. Cowan, G. Sciolla, F. Taylor, R. K. Yamamoto

Massachusetts Institute of Technology, Laboratory for Nuclear Science, Cambridge, MA 02139, USA

M. Milek, P. M. Patel

McGill University, Montréal, QC, Canada H3A 2T8

4

F. Palombo

Università di Milano, Dipartimento di Fisica and INFN, I-20133 Milano, Italy

J. M. Bauer, L. Cremaldi, V. Eschenburg, R. Kroeger, J. Reidy, D. A. Sanders, D. J. Summers

University of Mississippi, University, MS 38677, USA

C. Hast, P. Taras

Université de Montréal, Laboratoire René J. A. Lévesque, Montréal, QC, Canada H3C 3J7

H. Nicholson

Mount Holyoke College, South Hadley, MA 01075, USA

C. Cartaro, N. Cavallo, G. De Nardo, F. Fabozzi, C. Gatto, L. Lista, P. Paolucci, D. Piccolo, C. Sciacca

Università di Napoli Federico II, Dipartimento di Scienze Fisiche and INFN, I-80126, Napoli, Italy

J. M. LoSecco

University of Notre Dame, Notre Dame, IN 46556, USA

J. R. G. Alsmiller, T. A. Gabriel

Oak Ridge National Laboratory, Oak Ridge, TN 37831, USA

J. Brau, R. Frey, M. Iwasaki, C. T. Potter, N. B. Sinev, D. Strom, E. Torrence

University of Oregon, Eugene, OR 97403, USA

F. Colecchia, A. Dorigo, F. Galeazzi, M. Margoni, M. Morandin, M. Posocco, M. Rotondo, F. Simonetto, R. Stroili, C. Voci

Università di Padova, Dipartimento di Fisica and INFN, I-35131 Padova, Italy

M. Benayoun, H. Briand, J. Chauveau, P. David, Ch. de la Vaissière, L. Del Buono, O. Hamon, Ph. Leruste, J. Ocariz, M. Pivk, L. Roos, J. Stark

Universités Paris VI et VII, Lab de Physique Nucléaire H. E., F-75252 Paris, France

P. F. Manfredi, V. Re, V. Speziali

Università di Pavia, Dipartimento di Elettronica and INFN, I-27100 Pavia, Italy

L. Gladney, Q. H. Guo, J. Panetta

University of Pennsylvania, Philadelphia, PA 19104, USA

C. Angelini, G. Batignani, S. Bettarini, M. Bondioli, F. Bucci, G. Calderini, E. Campagna, M. Carpinelli, F. Forti, M. A. Giorgi, A. Lusiani, G. Marchiori, F. Martinez-Vidal, M. Morganti, N. Neri, E. Paoloni, M. Rama, G. Rizzo, F. Sandrelli, G. Triggiani, J. Walsh

Università di Pisa, Scuola Normale Superiore and INFN, I-56010 Pisa, Italy

M. Haire, D. Judd, K. Paick, L. Turnbull, D. E. Wagoner

Prairie View A&M University, Prairie View, TX 77446, USA

J. Albert, G. Cavoto,[2] N. Danielson, P. Elmer, C. Lu, V. Miftakov, J. Olsen, S. F. Schaffner, A. J. S. Smith, A. Tumanov, E. W. Varnes

Princeton University, Princeton, NJ 08544, USA

---

[2]Also with Università di Roma La Sapienza, Roma, Italy

F. Bellini, D. del Re, R. Faccini,[3] F. Ferrarotto, F. Ferroni, E. Leonardi, M. A. Mazzoni, S. Morganti,
G. Piredda, F. Safai Tehrani, M. Serra, C. Voena

Università di Roma La Sapienza, Dipartimento di Fisica and INFN, I-00185 Roma, Italy

S. Christ, G. Wagner, R. Waldi

Universität Rostock, D-18051 Rostock, Germany

T. Adye, N. De Groot, B. Franek, N. I. Geddes, G. P. Gopal, S. M. Xella

Rutherford Appleton Laboratory, Chilton, Didcot, Oxon, OX11 0QX, United Kingdom

R. Aleksan, S. Emery, A. Gaidot, P.-F. Giraud, G. Hamel de Monchenault, W. Kozanecki, M. Langer,
G. W. London, B. Mayer, G. Schott, B. Serfass, G. Vasseur, Ch. Yeche, M. Zito

DAPNIA, Commissariat à l'Energie Atomique/Saclay, F-91191 Gif-sur-Yvette, France

M. V. Purohit, A. W. Weidemann, F. X. Yumiceva

University of South Carolina, Columbia, SC 29208, USA

I. Adam, D. Aston, N. Berger, A. M. Boyarski, M. R. Convery, D. P. Coupal, D. Dong, J. Dorfan,
W. Dunwoodie, R. C. Field, T. Glanzman, S. J. Gowdy, E. Grauges , T. Haas, T. Hadig, V. Halyo,
T. Himel, T. Hryn'ova, M. E. Huffer, W. R. Innes, C. P. Jessop, M. H. Kelsey, P. Kim, M. L. Kocian,
U. Langenegger, D. W. G. S. Leith, S. Luitz, V. Luth, H. L. Lynch, H. Marsiske, S. Menke, R. Messner,
D. R. Muller, C. P. O'Grady, V. E. Ozcan, A. Perazzo, M. Perl, S. Petrak, H. Quinn, B. N. Ratcliff,
S. H. Robertson, A. Roodman, A. A. Salnikov, T. Schietinger, R. H. Schindler, J. Schwiening, G. Simi,
A. Snyder, A. Soha, S. M. Spanier, J. Stelzer, D. Su, M. K. Sullivan, H. A. Tanaka, J. Va'vra,
S. R. Wagner, M. Weaver, A. J. R. Weinstein, W. J. Wisniewski, D. H. Wright, C. C. Young

Stanford Linear Accelerator Center, Stanford, CA 94309, USA

P. R. Burchat, C. H. Cheng, T. I. Meyer, C. Roat

Stanford University, Stanford, CA 94305-4060, USA

R. Henderson

TRIUMF, Vancouver, BC, Canada V6T 2A3

W. Bugg, H. Cohn

University of Tennessee, Knoxville, TN 37996, USA

J. M. Izen, I. Kitayama, X. C. Lou

University of Texas at Dallas, Richardson, TX 75083, USA

F. Bianchi, M. Bona, D. Gamba

Università di Torino, Dipartimento di Fisica Sperimentale and INFN, I-10125 Torino, Italy

L. Bosisio, G. Della Ricca, S. Dittongo, L. Lanceri, P. Poropat, L. Vitale, G. Vuagnin

Università di Trieste, Dipartimento di Fisica and INFN, I-34127 Trieste, Italy

R. S. Panvini

Vanderbilt University, Nashville, TN 37235, USA

---

[3]Also with University of California at San Diego, La Jolla, CA 92093, USA

S. W. Banerjee, C. M. Brown, D. Fortin, P. D. Jackson, R. Kowalewski, J. M. Roney

University of Victoria, Victoria, BC, Canada V8W 3P6

H. R. Band, S. Dasu, M. Datta, A. M. Eichenbaum, H. Hu, J. R. Johnson, R. Liu, F. Di Lodovico,
A. Mohapatra, Y. Pan, R. Prepost, I. J. Scott, S. J. Sekula, J. H. von Wimmersperg-Toeller, J. Wu,
S. L. Wu, Z. Yu

University of Wisconsin, Madison, WI 53706, USA

H. Neal

Yale University, New Haven, CT 06511, USA

1 Introduction

The symmetry for combined charge conjugation *(C)* and parity *(P)* transformations is violated in B decays. Measurements of CP asymmetries by the *BABAR* [1] and BELLE [2] collaborations established this effect and are compatible with the Standard Model expectation based on the current knowledge of the Cabibbo-Kobayashi-Maskawa [3] quark-mixing matrix elements.

As a result of the interference between direct B decay, expected to be dominated by the tree decay diagram, and decay after flavor change, a CP-violating asymmetry is expected in the time evolution of the decays[4] $B^0 \to D^{*+}D^{*-}$, within the framework of the Standard Model [4]. Up to corrections due to theoretically uncertain penguin diagram contributions [5], this CP asymmetry is related to $\sin 2\beta$ ($\beta \equiv \arg[-V_{\rm cd}V_{\rm cb}^*/V_{\rm td}V_{\rm tb}^*]$). Penguin-induced corrections are predicted to be small in models based on the factorization approximation and heavy quark symmetry; an effect of about 2% is predicted by Ref. [6]. A comparison of measurements of $\sin 2\beta$ [7] from charmonium-containing $b \to c\bar{c}s$ modes such as $B^0 \to J/\psi K_S^0$, with that obtained in $B^0 \to D^{*+}D^{*-}$ is an important test of these models and the consistency of the Standard Model.

The $B^0 \to D^{*+}D^{*-}$ mode is a pseudoscalar decay to a vector-vector final state, with contributions from three partial waves with different CP parities: even for the S- and D-waves, odd for the P-wave. In the model described in Ref. [8] the P-wave contribution is predicted to be about 11%. The angular distribution of the decay products can be used to measure the CP parameters of the CP-even and CP-odd components [9].

Following our initial results on this channel [10], we present here an updated determination of the CP-odd fraction $R_\perp$ in the decay $B^0 \to D^{*+}D^{*-}$ in *BABAR*, based on a projected one-dimensional time-integrated angular analysis. We also present a preliminary measurement of the time-dependent CP asymmetry, obtained from a combined analysis of the time dependence of flavor-tagged decays and the one-dimensional angular distribution of decay products.

2 The *BABAR* Detector and Dataset

The data used in this analysis were collected with the *BABAR* detector at the PEP-II storage ring. The data sample used for the time-dependent CP-asymmetry measurement corresponds to 88.0×10^6 $e^+e^- \to \Upsilon(4S) \to B\bar{B}$ events and the sample used for the $R_\perp$ measurement corresponds to $84.4 \times 10^6 B\bar{B}$ pairs. The collider is operated with asymmetric beam energies, producing a boost ($\beta\gamma = 0.55$) of the $\Upsilon(4S)$ along the collision axis.

BABAR is a solenoidal detector optimized for the asymmetric beam configuration at PEP-II, and is described in detail elsewhere [11]. Charged particle (track) momenta are measured in a tracking system consisting of a 5-layer, double-sided, silicon vertex tracker (SVT) and a 40-layer drift chamber (DCH) filled with a gas mixture of helium and isobutane, both operating within a 1.5 T superconducting solenoidal magnet. Photon candidates are selected as local maxima of deposited energy in an electromagnetic calorimeter (EMC) consisting of 6580 CsI(Tl) crystals arranged in barrel and forward endcap subdetectors. In this analysis, tracks are identified as pions or kaons by the Cherenkov angle θ_c, measured using a detector of internally reflected Cherenkov light (DIRC), and by the energy deposition, dE/dx, in the tracking system. The flux return of the magnet is instrumented with resistive plate chambers interspersed with iron (IFR) for the identification of muons and long-lived neutral hadrons.

---

[4]Charge-conjugate modes are implied throughout this paper.

3 Event Selection

B^0 mesons are exclusively reconstructed by combining two charged D^* candidates reconstructed in a number of D^* and D decay modes. Events are pre-selected by requiring that the normalized second Fox-Wolfram moment [12] of the event be less than 0.6. We also require that the cosine of the angle between the thrust axis of the reconstructed B and the thrust axis of the rest of the event be less than 0.9. These criteria are used to reject events coming from the $e^+e^- \to c\bar{c}$ continuum process. Backgrounds from u, d, s continuum processes are negligible in this analysis due to the presence of two charm particles in the final state.

The D^0 and D^+ modes reconstructed are $D^0 \to K^-\pi^+$, $D^0 \to K^-\pi^+\pi^0$, $D^0 \to K^-\pi^+\pi^+\pi^-$, $D^0 \to K_S^0\pi^+\pi^-$, $D^+ \to K^-\pi^+\pi^+$, $D^+ \to K_S^0\pi^+$ and $D^+ \to K^-K^+\pi^+$.

Charged kaon candidates are required to be inconsistent with the pion hypothesis, as inferred from the Cherenkov angle measured by the DIRC and the specific ionization measured by the SVT and DCH. No particle identification requirements are made for the kaon from the decay $D^0 \to K^-\pi^+$.

$K_S^0 \to \pi^+\pi^-$ candidates are required to have an invariant mass within 25 MeV/c^2 of the nominal K_S^0 mass [13]. The angle between the flight direction and the momentum vector of the K_S^0 candidate is required to be less than 200 mrad, and the transverse flight distance from the primary event vertex must be greater than 2 mm. A mass-constrained fit is then applied to each surviving K_S^0 candidate, in order to improve the mass resolution of the $K_S^0\pi^+$ and $K_S^0\pi^+\pi^-$ combinations.

Neutral pion candidates are formed from two photons in the EMC, each with energy above 30 MeV; the invariant mass of the pair must be within 20 MeV/c^2 of the nominal π^0 mass, and their summed energy must be greater than 200 MeV. A mass-constrained fit is then applied to these π^0 candidates. The π^0 from $D^{*+} \to D^+\pi^0$ decay ("soft" π^0), however, is required to have an invariant mass within 35 MeV/c^2 of the nominal π^0 mass and momentum in the $\Upsilon(4S)$ frame in the interval $70 < |p^*| < 450$ MeV/c, with no requirement on the photon energy sum.

D^0 and D^+ meson candidates are required to have an invariant mass within 20 MeV/c^2 of the nominal D^0 or D^+ mass. The same interval is used for all D^0 modes except $K^-\pi^+\pi^0$, which has a looser requirement of 35 MeV/c^2 due to the momentum resolution of the π^0.

D^{*+} mesons are reconstructed in their decays $D^{*+} \to D^0\pi^+$ and $D^{*+} \to D^+\pi^0$. We include $D^{*+}D^{*-}$ combinations decaying to $(D^0\pi^+, \overline{D}^0\pi^-)$ or $(D^0\pi^+, D^-\pi^0)$, but not $(D^+\pi^0, D^-\pi^0)$ due to the smaller branching fraction and larger expected backgrounds. The D^0 and D^+ candidates are subjected to a mass-constrained fit and then combined with soft pion candidates. A vertex fit is performed that includes the position of the beam spot to improve the angular resolution of the soft pion.

If an event contains both a D^{*+} and a D^{*-} candidate, each is subjected to a mass constraint fit, and then combined to form a B candidate. B^0 candidates with well reconstructed D^* and D mesons are selected by means of a mass likelihood variable, $\mathcal{L}_{Mass}$, that includes all measured D^* and D masses. This variable is defined in Eq. 1:

$$\mathcal{L}_{Mass} = G(m_D;\ m_{D_{PDG}}, \sigma_{m_D}) \times G(m_{\bar{D}};\ m_{D_{PDG}}, \sigma_{m_{\bar{D}}}) \times$$
$$\left[f_{core}\ G(\Delta m_{D^{*+}};\ \Delta m_{D^*_{PDG}}, \sigma_{\Delta m_{core}}) \right.$$
$$+ \quad (1 - f_{core})\ G(\Delta m_{D^{*+}};\ \Delta m_{D^*_{PDG}}, \sigma_{\Delta m_{tail}}) \Big] \times$$
$$\left[f_{core}\ G(\Delta m_{D^{*-}};\ \Delta m_{D^*_{PDG}}, \sigma_{\Delta m_{core}}) \right.$$
$$+ \quad (1 - f_{core})\ G(\Delta m_{D^{*-}};\ \Delta m_{D^*_{PDG}}, \sigma_{\Delta m_{tail}}) \Big] \qquad (1)$$

where $G(x; \mu, \sigma)$ is a normalized Gaussian defined with mean $= \mu$ and RMS $= \sigma$; the subscript PDG refers to the nominal value [13]. For σ_{m_D} we use errors calculated candidate-by-candidate. The parameter f_{core} is the ratio of areas for the core and tail Gaussians. This along with $\sigma_{\Delta m_{core}}$ and $\sigma_{\Delta m_{tail}}$ are determined from fitting the Δm distributions in simulated signal events. The value of $-\ln(\mathcal{L}_{Mass})$ is used to select signal in preference to background, with a different requirement used for each D decay mode combination. In an event where more than one B candidate is reconstructed, the candidate with the lowest $-\ln(\mathcal{L}_{Mass})$ value is chosen.

The primary variables used to distinguish signal from background are the energy-substituted mass,

$$m_{\mathrm{ES}} \equiv \sqrt{E^*_{Beam}{}^2 - p^*_B{}^2}$$

and the difference of the B candidate energy from beam energy,

$$\Delta E \equiv E^*_B - E^*_{Beam}$$

where the star indicates variables evaluated in the $\Upsilon(4S)$ center-of-mass frame. The fits described in the following sections are performed on events required to have $|\Delta E| < 25\,\mathrm{MeV}$ and $m_{\mathrm{ES}} > 5.2\,\mathrm{GeV}/c^2$. The requirements on $-\ln(\mathcal{L}_{Mass})$ and ΔE were chosen to optimize $S^2/(S + B)$, where S is the expected number of signal events and B is the expected number of background events. The optimization process was done with samples of simulated signal events and with generic $B\bar{B}$ and $c\bar{c}$ Monte Carlo simulated events.

Figure 1 shows the events in the m_{ES} projection after all selection criteria have been applied. The fit to this distribution uses a Gaussian and an ARGUS function [14] parameterization for signal and background, respectively. For the data sample corresponding to $84.4 \times 10^6 B\bar{B}$ pairs, the fitted signal yield is $126 \pm 13\ D^{*+}D^{*-}$ events.

4 Measurement of the CP-odd Fraction in $B^0 \rightarrow D^{*+}D^{*-}$

In this section we present a one-dimensional angular analysis to determine the fraction, $R_\perp$, of the P-wave CP-odd component in the vector-vector final state of the $B^0 \rightarrow D^{*+}D^{*-}$ decay. In the transversity basis [9] the following three angles involving decay products are defined (see Fig. 2):

- the polar angle θ_1 between the momentum of the π^- in the D^{*-} rest frame, and the direction of flight of the D^{*-} in the B rest frame,

- the polar angle θ_{tr} between the normal, z, to the D^{*-} decay plane and the π^+ line of flight in the D^{*+} rest frame, and
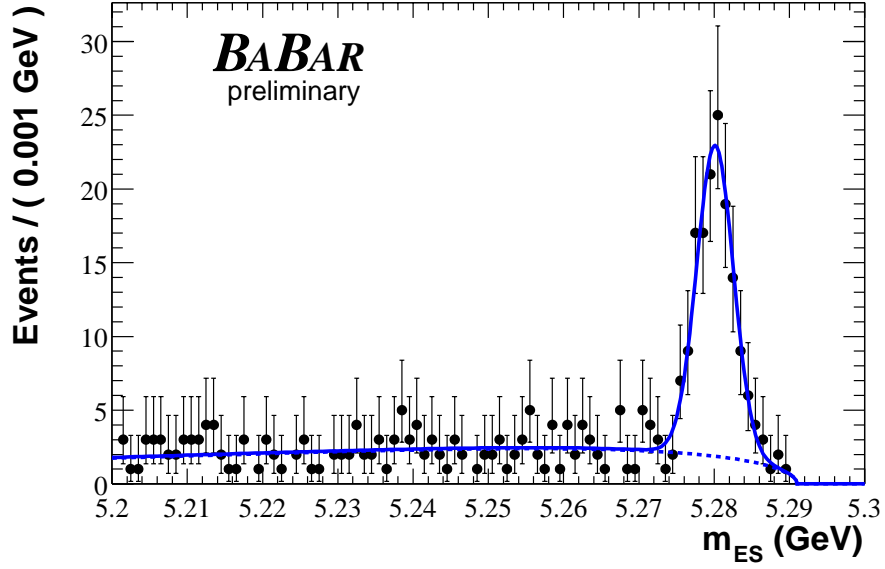
- the corresponding azimuthal angle ϕ_{tr}.

10

Figure 1: The m_{ES} projection of the data for $B^0 \to D^{*+}D^{*-}$. These events are required to have $|\Delta E| < 25\,\text{MeV}$. The solid (dashed) line represents the result (background component) of the fit described in the text.
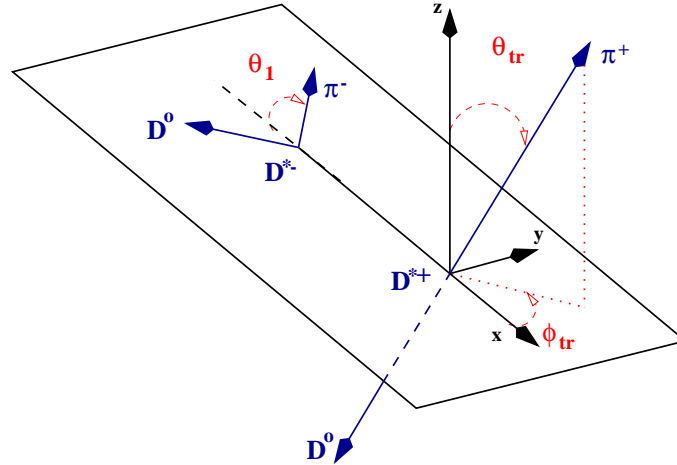

Figure 2: Representation of the "Transversity Frame" for the decay $B^0 \to D^{*+}D^{*-}$. The momenta of the D^{*-} decay products are represented in the B^0 rest frame, while the momenta of the D^{*+} decay products are represented in the D^{*+} rest frame. The x direction is defined by the direction of flight of the D^{*+} in the B^0 rest frame. The (x, y) plane is defined by the momenta of the D^{*-} decay products in the B^0 rest frame. The "transversity" axis, z, is orthogonal to the (x, y) plane.

The time-dependent angular distribution of decay products in the transversity frame for the mode $B^0 \to D^{*+}D^{*-}$ is given by [15][5]:

$$\frac{1}{\Gamma}\frac{\mathrm{d}^4\Gamma}{\mathrm{d}\cos\theta_1\mathrm{d}\cos\theta_{\mathrm{tr}}\mathrm{d}\phi_{\mathrm{tr}}\mathrm{dt}} = \frac{9}{32\pi}\frac{1}{|A_0|^2+|A_\parallel|^2+|A_\perp|^2}$$

$$\{4|A_0|^2\cos^2\theta_1\sin^2\theta_{\mathrm{tr}}\cos^2\phi_{\mathrm{tr}}$$

$$+2|A_\parallel|^2\sin^2\theta_1\sin^2\theta_{\mathrm{tr}}\sin^2\phi_{\mathrm{tr}}$$

$$+2|A_\perp|^2\sin^2\theta_1\cos^2\theta_{\mathrm{tr}}$$

$$+\sqrt{2}\mathrm{Re}(A_\parallel^*A_0)\sin 2\theta_1\sin^2\theta_{\mathrm{tr}}\sin 2\phi_{\mathrm{tr}}$$

$$-\sqrt{2}\mathrm{Im}(A_0^*A_\perp)\sin 2\theta_1\sin 2\theta_{\mathrm{tr}}\cos\phi_{\mathrm{tr}}$$

$$-2\mathrm{Im}(A_\parallel^*A_\perp)\sin^2\theta_1\sin 2\theta_{\mathrm{tr}}\sin\phi_{\mathrm{tr}}\} . \tag{2}$$

where $A_0, A_\parallel, A_\perp$ are the time-dependent decay amplitudes in the transversity basis. For the $\bar{B}^0$ decay $\bar{A}_\perp = -A_\perp$, under the assumption there is no direct CP violation.

In principle, 11 unknown parameters can be extracted from a full angular, time, and B-flavor dependent analysis. These parameters are: $M_i \equiv |A_i(t=0)|$, 2 relative phases, and the complex CP parameters $\lambda_i = (q/p)(\bar{A}_i/A_i)$, with $i = \parallel, 0, \perp$, resulting from the interference of mixing (q/p) and decay amplitudes (A_i). Considering the size of the current data sample, a simplified strategy is adopted to extract only the CP-odd component from the $\cos\theta_{\mathrm{tr}}$ distribution.

Ignoring the B flavor and integrating over time, θ_1, and ϕ_{tr} results in the one-dimensional differential decay rate:

$$\frac{1}{\Gamma}\frac{\mathrm{d}\Gamma}{\mathrm{d}\cos\theta_{\mathrm{tr}}} = \frac{3}{4}(1-R_\perp)\sin^2\theta_{\mathrm{tr}} + \frac{3}{2}R_\perp\cos^2\theta_{\mathrm{tr}} \tag{3}$$

with:

$$R_\perp = \frac{M_\perp^2}{M_0^2 + M_\parallel^2 + M_\perp^2} . \tag{4}$$

The measurement of $R_\perp$ is based on an unbinned maximum likelihood fit of the $\cos\theta_{\mathrm{tr}}$ distribution, with a simultaneous fit to the m_{ES} distribution. The probability density function for the m_{ES} distribution is given by the sum of normalized ARGUS [14] and Gaussian functions; the relative weight of each function is given by a signal fraction f_{sig}, which is allowed to float in the likelihood fit. The likelihood is defined as:

$$\mathcal{L} = \prod_{i=1,n} \Big[f_{sig}\times\mathcal{F}_{m\mathrm{ES}}^{sig}(m_{\mathrm{ES},i};\sigma_{m_{ES}})\times\mathcal{F}_{R_\perp}(\cos\theta_i;R_\perp)+$$

$$(1-f_{sig})\times\mathcal{F}_{m\mathrm{ES}}^{bkg}(m_{\mathrm{ES},i};\kappa)\times\mathcal{F}_{bkg}(\cos\theta_i;b_2)\Big], \tag{5}$$

where n is the number of selected events in the m_{ES} distribution, $\mathcal{F}_{m\mathrm{ES}}^{sig}$ is the signal Gaussian for the m_{ES} distribution and $\mathcal{F}_{m\mathrm{ES}}^{bkg}$ is the background ARGUS function with shape parameter κ. $\mathcal{F}_{R_\perp}$

---

[5]Eq.5.44 in the reference appears with wrong signs in the last two terms and has been corrected in Eq. 2 of this paper.

refers to the probability density function for signal events, given by Eq. 3. The background shape is modeled by a polynomial in $\cos\theta_{tr}$:

$$\mathcal{F}_{bkg}(\cos\theta_{tr}; b_2) = N \times (1 + b_2\cos^2\theta_{tr}), \qquad (6)$$

where N is the normalization factor.

We categorize our events in three types: $D^{*+}D^{*-} \rightarrow (D^0\pi^+, \overline{D}^0\pi^-)$, $(D^0\pi^+, D^-\pi^0)$, and $(D^+\pi^0, \overline{D}^0\pi^-)$. We distinguish these three types of events because events with a neutral slow pion and events with a charged slow pion have different background levels and $\cos\theta_{tr}$ resolution (note: θ_{tr} is the angle between the slow pion from the D^{*+} and the transversity axis).

We allow different signal fractions for each event type. Thus, the parameters floating in the likelihood fit are: 3 signal fractions, the background parameter b_2, 3 m_{ES} parameters (σ and mean of Gaussian fit, and κ from ARGUS shape), and $R_\perp$.

A fit to the dataset yields a value of $R_\perp = 0.096 \pm 0.060(stat)$, neglecting possible biases from angular resolution in θ_{tr} and detector acceptance. Figure 3 shows the distribution of $\cos\theta_{tr}$ for candidates with m_{ES} in the range $m_{ES} > 5.27$ GeV/c^2, with the result of the fit projected in the same region. The background component of the pdf is shown as the dotted line.
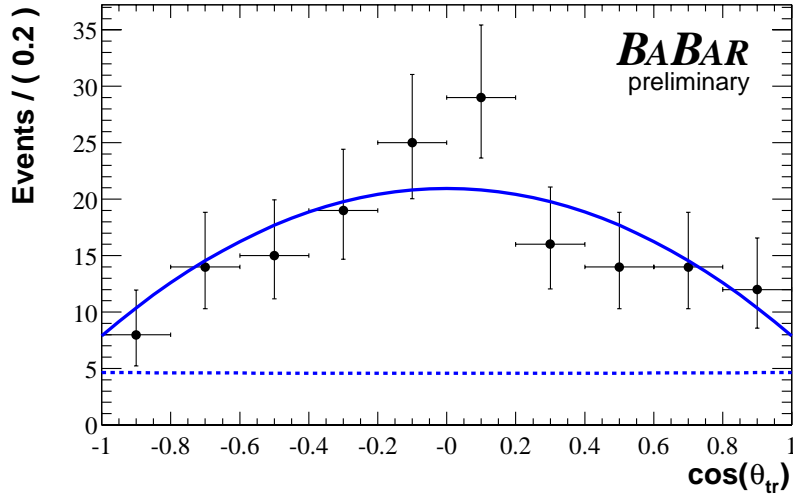

Figure 3: Likelihood fit result to the $\cos\theta_{tr}$ distribution of the $D^{*+}D^{*-}$ events. The data points shown are from the region $m_{ES} > 5.27$ GeV/c^2 and the solid line is the projection of the fit result in the same region. The dotted line represents the component of the pdf for the background.

The experimental resolution of θ_{tr} biases the measurement of $R_\perp$; the simulated distribution of residuals on θ_{tr} is seen to have significant tails caused by mis-reconstructed events. The presence of these tails distorts the $\cos\theta_{tr}$ distribution, and thus produces a bias on $R_\perp$. A smaller bias on $R_\perp$ is produced by the transverse momentum dependence of the detector reconstruction efficiency. The presence of the two slow pions from the D^* decays makes this analysis susceptible to this effect. The net bias from these two effects was estimated from a study on simulated data, and is found to be +0.028. This was determined using simulated events with a generated value of $R_\perp$ very similar to the value measured in data. The corresponding systematic error incurred for this correction is taken conservatively to be the full size of the correction, namely 0.028. The next largest systematic

uncertainty affecting the $R_\perp$ measurement arises from the background parameterization (0.005). The total systematic uncertainty on $R_\perp$ is determined to be 0.03, giving as a preliminary result the final corrected value:

$$R_\perp = 0.07 \pm 0.06(stat) \pm 0.03(syst). \tag{7}$$

This is an update to a previous *BABAR* measurement [10], with a factor of three reduction in the statistical error ($R_\perp$ dependent).

5 Measurement of the Time-Dependent CP Asymmetry in $B^0 \to D^{*+}D^{*-}$

In this section we present a determination of the time-dependent CP asymmetry in $B^0 \to D^{*+}D^{*-}$. We perform a combined analysis of the $\cos\theta_{\rm tr}$ distribution of all selected events and the time dependence of those with a flavor tag. The inclusion of the angular dependence enables us to fit for the CP asymmetries of the CP-even and CP-odd components separately.

Although factorization models predict a small penguin contamination of the weak phase difference $\text{Im}(\lambda_f) = -\sin 2\beta$ [6], a sizeable penguin diagram contribution cannot *a priori* be excluded. Thus, the value of $\lambda_f = \frac{q}{p}\frac{\bar{A}(f)}{A(f)}$ can be different for the three transversity amplitudes because of possible different penguin-to-tree ratios. These contributions are explicitly included in the parameterization of the flavor-tagged decay rates described here.

The decay rate, $f_+(f_-)$, for a neutral B meson tagged as a $B^0(\bar{B}^0)$ can be obtained from Eq. 2 as:

$$f_\pm(\Delta t) = \frac{e^{-|\Delta t|/\tau_{B^0}}}{4\tau_{B^0}}\left\{O(1 - \tfrac{1}{2}\Delta\mathcal{D}) \mp \mathcal{D}\left[S\sin\left(\Delta m_d\Delta t\right) + C\cos\left(\Delta m_d\Delta t\right)\right]\right\}, \tag{8}$$

where $\Delta t = t_{\rm rec} - t_{\rm tag}$ is the difference between the proper decay time of the reconstructed B meson ($B_{\rm rec}$) and the proper decay time of the tagging B meson ($B_{\rm tag}$), τ_{B^0} is the B^0 lifetime, and Δm_d is the mass difference determined from the B^0-$\bar{B}^0$ oscillation frequency. The dilution factor, $\mathcal{D}$, describes the effect of incorrect tags, with $\Delta\mathcal{D}$ accounting for possible differences in the mis-tag probability between B^0 and $\bar{B}^0$. The O, C and S coefficients are defined as:

$$
\begin{aligned}
O &= \frac{3}{4}[(1 - R_\perp)\sin^2\theta_{\rm tr} + 2R_\perp\cos^2\theta_{\rm tr}] \\
C &= \frac{3}{4}[(1 - R_\perp)\frac{1 - |\lambda_+|^2}{1 + |\lambda_+|^2}\sin^2\theta_{\rm tr} + 2R_\perp\frac{1 - |\lambda_\perp|^2}{1 + |\lambda_\perp|^2}\cos^2\theta_{\rm tr}] \\
S &= -\frac{3}{4}[(1 - R_\perp)\frac{2\text{Im}(\lambda_+)}{1 + |\lambda_+|^2}\sin^2\theta_{\rm tr} - 2R_\perp\frac{2\text{Im}(\lambda_\perp)}{1 + |\lambda_\perp|^2}\cos^2\theta_{\rm tr}].
\end{aligned}
\tag{9}
$$

These coefficients contain the explicit dependence on the transversity angle $\theta_{\rm tr}$ defined in the previous section, which provides a separation between the CP-odd ($\cos^2\theta_{\rm tr}$) and CP-even ($\sin^2\theta_{\rm tr}$) components.

The CP-even parameters, $|\lambda_+|$ and $\text{Im}(\lambda_+)$, are related to $\lambda_\parallel$ and λ_0 by:

Table 1: Efficiencies ϵ_i, average mis-tag fractions w_i, mis-tag fraction differences $\Delta w_i = w_i(B^0) - w_i(\overline{B}^0)$, and Q extracted for each tagging category i by using the B_{flav} sample.

Category	ε (%)	w (%)	Δw (%)	Q (%)
Lepton	9.1 ± 0.2	3.3 ± 0.6	-1.5 ± 1.1	7.9 ± 0.3
Kaon I	16.7 ± 0.2	10.0 ± 0.7	-1.3 ± 1.1	10.7 ± 0.4
Kaon II	19.8 ± 0.3	20.9 ± 0.8	-4.4 ± 1.2	6.7 ± 0.4
Inclusive	20.0 ± 0.3	31.5 ± 0.9	-2.4 ± 1.3	2.7 ± 0.3
All	65.6 ± 0.5			28.1 ± 0.7

$$\frac{1 - |\lambda_+|^2}{1 + |\lambda_+|^2} = \frac{\frac{1-|\lambda_\||^2}{1+|\lambda_\||^2}M_\|^2 + \frac{1-|\lambda_0|^2}{1+|\lambda_0|^2}M_0^2}{M_\|^2 + M_0^2}$$

$$\frac{\text{Im}(\lambda_+)}{1 + |\lambda_+|^2} = \frac{\frac{\text{Im}(\lambda_\|)}{1+|\lambda_\||^2}M_\|^2 + \frac{\text{Im}(\lambda_0)}{1+|\lambda_0|^2}M_0^2}{M_\|^2 + M_0^2}. \tag{10}$$

It should be noted that this formulation does not take into account detector acceptance. Therefore, a combined fit to the Δt and $\cos\theta_{\text{tr}}$ dependence of the data will give an "effective" value of $R_\perp$, which is not necessarily identical to the acceptance-corrected value from the time-integrated measurement.

A measurement of CP asymmetries requires a determination of the experimental Δt resolution and the fraction of events in which the tag assignment is incorrect. A mis-tag fraction w reduces the observed CP asymmetry by a factor $\mathcal{D} = 1 - 2w$. The mis-tag fractions and Δt resolution functions are determined from a sample, B_{flav}, of neutral B decays to flavor eigenstates $(D^{(*)-}h^+(h^+ = \pi^+, \rho^+, \text{and } a_1^+)$ and $J/\psi K^{*0}(K^{*0} \to K^+\pi^-))$ as for the $\sin2\beta$ measurement using charmonium decays, described in detail elsewhere [7].

We use multivariate algorithms to identify signatures of B decays that determine the flavor of B_{tag}. Primary leptons from semileptonic B decays are selected from identified electrons, muons, and isolated energetic tracks. We use the charges of the best kaon candidates to define a kaon tag. Soft pions from D^{*+} decays are selected on the basis of their momentum and direction with respect to the thrust axis of B_{tag}. A neural network, which combines the outputs of these algorithms, takes into account correlations between different sources of flavor information and provides an estimate of the mis-tag probability for each event.

Using the outputs of the algorithms and the estimated mis-tag probability, each event is assigned to one of four hierarchical, mutually exclusive tagging categories. The Lepton category contains events with an identified lepton, and a supporting kaon tag if present. Events with a kaon candidate and soft pion with opposite charge and similar flight direction are assigned to the Kaon I category. Events with only a kaon tag are assigned to the Kaon I or Kaon II category depending on the estimated mis-tag probability. The Kaon II category also contains the remaining events with a soft pion. All other events are assigned to the Inclusive category or excluded from further analysis based on the estimated mis-tag probability. The tagging efficiencies ε_i for the four tagging categories are measured from data and summarized in Table 1. The figure of merit for tagging is the effective tagging efficiency $Q \equiv \sum_i \varepsilon_i(1 - 2w_i)^2$. This algorithm improves Q by about 7% (relative) over the

algorithm used in Ref. [16].

The algorithm for vertex reconstruction and the determination of Δt are described in detail in Ref. [16]. The time interval Δt between the two B decays is calculated from the measured separation Δz between the decay vertex of the reconstructed B meson and the vertex of the flavor-tagging B meson along the collision axis. We determine the z position of the B_{rec} vertex from the charged tracks that constitute the B_{rec} candidate. The decay vertex of the B_{tag} is determined by fitting the tracks not belonging to the B_{rec} candidate to a common vertex. An additional constraint on the tagging vertex comes from a pseudotrack computed from the B_{rec} vertex and three-momentum, the beam-spot and the $\Upsilon(4S)$ momentum. Events with a Δt error of less than 2.5 ps, and a measured $|\Delta t| < 20$ ps are accepted.

We determine the parameters $\mathrm{Im}(\lambda_+)$ and $|\lambda_+|$ with a simultaneous unbinned maximum likelihood fit to the Δt distributions of the B_{rec} and B_{flav} tagged samples (Fig. 4). The Δt distribution of the B_{flav} sample evolves according to the known frequency for flavor oscillations in neutral B mesons. The observed amplitudes for the CP asymmetry in the B_{rec} sample and for flavor oscillation in the B_{flav} sample are reduced by the same factor $(1 - 2w)$ due to flavor mis-tags. The Δt distributions for the B_{rec} and B_{flav} samples are both convolved with a common Δt resolution function. Events are assigned signal and background probabilities based on their m_{ES} values. Backgrounds are incorporated with an empirical description of their Δt evolution, containing prompt (zero lifetime) and non-prompt components convolved with a separate resolution function [16].

A total of 38 parameters are varied in the fit, including the values of $\mathrm{Im}(\lambda_+)$ and $|\lambda_+|$ (2), the effective CP-odd fraction (1), the average mis-tag fraction w and the difference Δw between B^0 and $\overline{B}^0$ mis-tags for each tagging category (8), parameters for the signal Δt resolution (9), and parameters for the background time dependence (7), Δt resolution (3), and mis-tag fractions (8). Because the CP-odd fraction is small, the parameters $|\lambda_\perp|$ and $\mathrm{Im}(\lambda_\perp)$ are poorly determined. Therefore they are fixed in the fit to 1.0 and -0.741 [7] respectively. These are the values expected if direct CP violation and contributions from penguin diagrams are neglected. The changes in the fitted values of $\mathrm{Im}(\lambda_+)$ and $|\lambda_+|$ for different input values of $\mathrm{Im}(\lambda_\perp)$ (varied between -1.0 and 1.0) and $|\lambda_\perp|$ (varied between 0.7 and 1.3) are taken into account as systematic uncertainties. The preliminary results obtained from the fit (Fig. 4) are as follows:

$$\mathrm{Im}(\lambda_+) = 0.31 \pm 0.43(stat) \pm 0.13(syst) \tag{11}$$

$$|\lambda_+| = 0.98 \pm 0.25(stat) \pm 0.09(syst). \tag{12}$$

The dominant source of systematic uncertainty comes from the variation on the value of $\lambda_\perp$ (0.09 and 0.02 respectively for $\mathrm{Im}(\lambda_+)$ and $|\lambda_+|$). Other relevant sources are the angular acceptance and resolution of the detector (0.06 and 0.08), the level, composition, and CP asymmetry of the background (0.07 and 0.02), the uncertainty on the SVT internal alignment and boost (0.03 and 0.02), limited Monte Carlo simulation statistics (0.02 and 0.01), and possible differences between B_{flav} and B_{rec} mis-tag fractions and resolution function parameters (0.01 and 0.01). The total systematic error is 0.13 for $\mathrm{Im}(\lambda_+)$ and 0.09 for $|\lambda_+|$.

If the $B \to D^{*+}D^{*-}$ transition proceeds only through the $b \to c\bar{c}d$ tree amplitude, we expect that $\mathrm{Im}(\lambda_+) = -\sin 2\beta$ and $|\lambda_+| = 1$. To test this hypothesis, we fix $\mathrm{Im}(\lambda_+) = -0.741$ [7] and $|\lambda_+| = 1$ and repeat the fit. The observed change in the likelihood corresponds to 2.7 standard deviations (statistical error only). More data is needed to establish whether there are significant contributions from other processes, in particular, penguin diagrams.
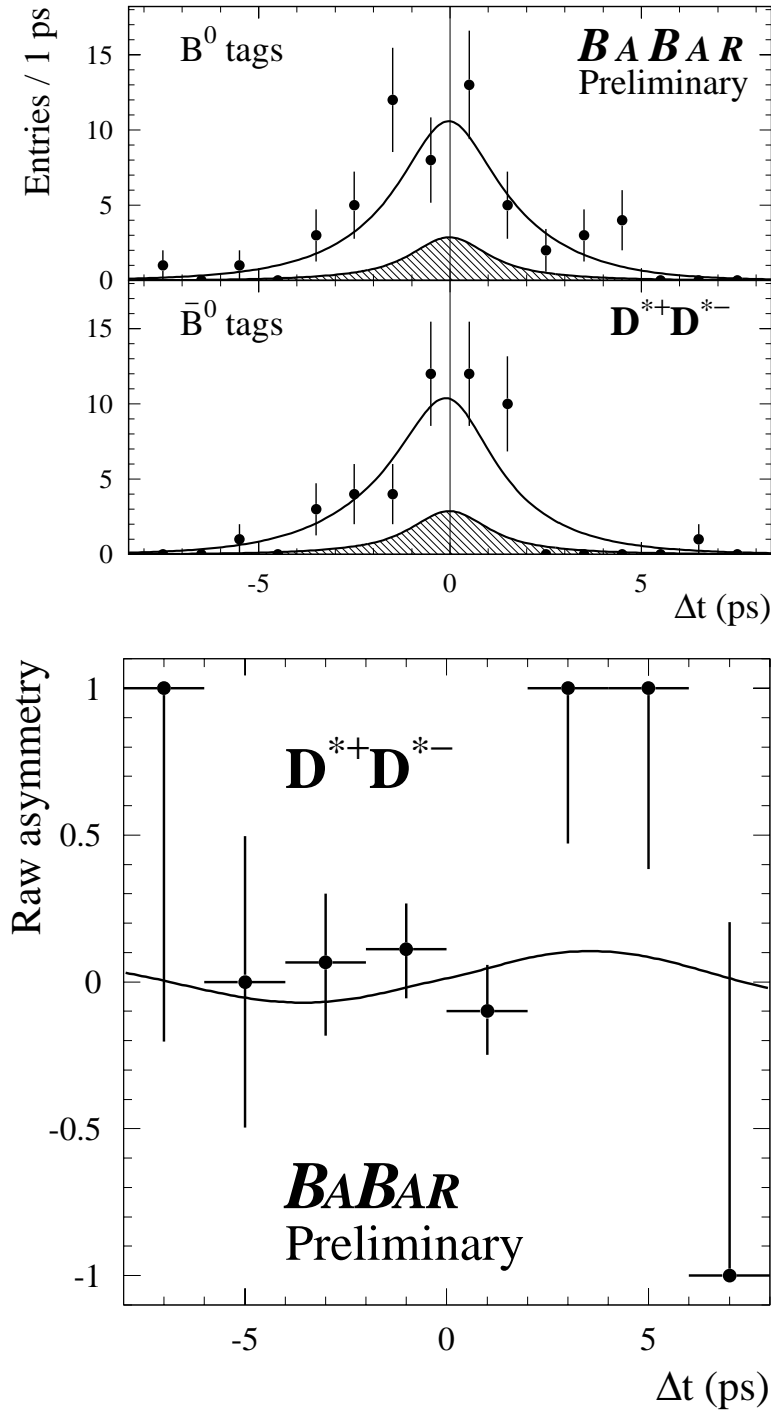
16

Figure 4: From top to bottom: number N_{B^0} of candidate events in the signal region with a B^0 tag, number $N_{\overline{B}^0}$ of candidates with a $\overline{B}^0$ tag, and the raw asymmetry $(N_{B^0} - N_{\overline{B}^0})/(N_{B^0} + N_{\overline{B}^0})$, as functions of Δt. The solid curves represent the result of the combined fit to the full sample. The shaded regions represent the background contributions.

6 Summary

We have reported preliminary measurements of time-dependent CP asymmetries and a measurement of the CP-odd fraction for the decay $B^0 \to D^{*+}D^{*-}$. The measurement of $R_\perp$ represents an improvement in the statistical uncertainty by a factor of almost three compared to previous measurements. The time-dependent asymmetry measurements still have large statistical uncertainties. These should be reduced steadily in the coming years as *BABAR* accumulates additional data, thus allowing useful tests of the Standard Model.

7 Acknowledgments

References

[1] B. Aubert, *et al.*, Phys. Rev. Lett. **87**, 091801 (2001).

[2] K. Abe, *et al.*, Phys. Rev. Lett. **87**, 091802 (2001).

[3] N. Cabibbo, Phys. Rev. Lett. **10**, 531 (1963);
M. Kobayashi and T. Maskawa, Prog. Th. Phys. **49**, 652 (1973).

[4] R. Aleksan, *et al.*, Phys. Lett. B **317**, 173 (1993).

[5] A.I. Sanda and Z.Z. Xing, Phys. Rev. D **56**, 341 (1997).

[6] X.Y. Pham and Z.Z. Xing, Phys. Rev. B **458**, 375 (1999).

[7] *BABAR* Collaboration, B. Aubert *et al.*, SLAC-PUB-9293, hep-ex/0207042, submitted to Phys. Rev. Lett.

[8] Z.Z. Xing, Phys. Rev. D **61**, 014010 (2000).

[9] I. Dunietz, *et al.*, Phys. Rev. D **43**, 2193 (1991).

[10] B. Aubert, *et al.*, SLAC-PUB-9152, hep-ex/0203008, to appear in Phys. Rev. Lett.

[11] The *BABAR* Collaboration, A. Palano *et al.*, Nucl. Intrum. Methods. **A479**, 1 (2002).

[12] G. C. Fox and S. Wolfram, Phys. Rev. Lett. **41**, 1581 (1978).

[13] Particle Data Group, K. Hagiwara *et al.*, Phys. Rev. D **66**, 010001 (2002).

[14] Defined as $A \sim \sqrt{1 - (m_{ES}/m_0)^2} \times \exp(\kappa(1 - (m_{ES}/m_0)^2)$ for $m_{ES} < m_0$. The value of m_0 is fixed to 5.291 GeV/c^2. ARGUS Collaboration, H. Albrecht *et al.*, Z. Phys. C **48**, 543 (1990).

[15] P. F. Harrison and H. R. Quinn, eds. "The *BABAR* Physics Book", SLAC-R504 (1998), Chapter 5, and references therein.

[16] *BABAR* Collaboration, B. Aubert *et al.*, SLAC-PUB-9060, hep-ex/0201020, to appear in Phys. Rev. D **.**